

## PTF10FQS: A LUMINOUS RED NOVA IN THE SPIRAL GALAXY MESSIER 99

MANSI M. KASLIWAL, SHRI R. KULKARNI,  
Cahill Center for Astrophysics, California Institute of Technology, Pasadena, CA, 91125, USA

IAIR ARCAVI,  
Benozio Center for Astrophysics, Faculty of Physics, The Weizmann Institute of Science, Rehovot 76100, Israel

ROBERT M. QUIMBY, ERAN O. OFEK,  
Cahill Center for Astrophysics, California Institute of Technology, Pasadena, CA, 91125, USA

PETER NUGENT, JANET JACOBSEN,  
Computational Cosmology Center, Lawrence Berkeley National Laboratory, 1 Cyclotron Road, Berkeley, CA 94720, USA

AVISHAY GAL-YAM, YOAV GREEN, OFER YARON,  
Benozio Center for Astrophysics, Faculty of Physics, The Weizmann Institute of Science, Rehovot 76100, Israel

DEREK B. FOX, JACOB L. HOWELL,  
Astronomy and Astrophysics, Eberly College of Science, The Pennsylvania State University, University Park, PA 16802, USA

S. BRADLEY CENKO, IO KLEISER, JOSHUA S. BLOOM, ADAM MILLER, WEIDONG LI, ALEXEI V. FILIPPENKO, DAN STARR,  
Department of Astronomy, University of California, Berkeley, CA 94720-3411, USA

DOVI POZNANSKI,  
Department of Astronomy, University of California, Berkeley, CA 94720-3411, USA and  
Computational Cosmology Center, Lawrence Berkeley National Laboratory, 1 Cyclotron Road, Berkeley, CA 94720, USA

NICHOLAS M. LAW,  
Dunlap Institute for Astronomy and Astrophysics, University of Toronto, 50 St. George Street, Toronto M5S 3H4, Ontario, Canada

GEORGE HELOU,  
Infrared Processing and Analysis Center, California Institute of Technology, Pasadena, CA 91125, USA

DALE A. FRAIL,  
National Radio Astronomy Observatory, Array Operations Center, Socorro, NM 87801, USA

JAMES D. NEILL, KARL FORSTER, D. CHRISTOPHER MARTIN, SHRIHARSH P. TENDULKAR,  
Cahill Center for Astrophysics, California Institute of Technology, Pasadena, CA, 91125, USA

NEIL GEHRELS,  
NASA-Goddard Space Flight Center, Greenbelt, MD 20771, USA

JAMIE KENNEA,  
Department of Astronomy and Astrophysics, Pennsylvania State University, State College, PA 16802, USA

MARK SULLIVAN,  
Department of Physics, Oxford University, Oxford, OX1 3RH, UK

LARS BILDSTEN,  
Kavli Institute of Theoretical Physics, University of California Santa Barbara, Santa Barbara, CA 93106, USA and

Department of Physics, University of California Santa Barbara, Santa Barbara, CA 93106, USA

RICHARD DEKANY, GUSTAVO RAHMER, DAVID HALE, ROGER SMITH, JEFF ZOLKOWER, VISWA VELUR, RICHARD WALTERS,  
JOHN HENNING, KAHNH BUI, DAN MCKENNA,  
Caltech Optical Observatories, California Institute of Technology, Pasadena, CA 91125, USA

CULLEN BLAKE

Department of Astrophysical Sciences, Princeton University, Princeton, NJ 08544, USA  
*Draft version March 29, 2011*

## ABSTRACT

The Palomar Transient Factory (PTF) is systematically charting the optical transient and variable sky. A primary science driver of PTF is building a complete inventory of transients in the local Universe (distance less than 200 Mpc). Here, we report the discovery of PTF 10fq, a transient in the luminosity “gap” between novae and supernovae. Located on a spiral arm of Messier 99, PTF 10fq has a peak luminosity of  $M_r = -12.3$ , red color ( $g - r = 1.0$ ) and is slowly evolving (decayed by 1 mag in 68 days). It has a spectrum dominated by intermediate-width  $H\alpha$  ( $\approx 930 \text{ km s}^{-1}$ ) and narrow calcium emission lines. The explosion signature (the light curve and spectra) is overall similar to that of M85 OT2006-1, SN 2008S, and NGC 300 OT. The origin of these events is shrouded in mystery and controversy (and in some cases, in dust). PTF 10fq shows some evidence of a broad feature (around  $8600 \text{ \AA}$ ) that may suggest very large velocities ( $\approx 10,000 \text{ km s}^{-1}$ ) in this explosion. Ongoing surveys can be expected to find a few such events per year. Sensitive spectroscopy, infrared monitoring and statistics (e.g. disk versus bulge) will eventually make it possible for astronomers to unravel the nature of these mysterious explosions.

*Subject headings:* stars: mass-loss — stars: AGB and post-AGB — supernovae: general — transients: individual (PTF 10fq)

## 1. INTRODUCTION

Two reasons motivate us to search for transients in the local Universe (distance  $< 200 \text{ Mpc}$ ). First, the emerging areas of gravitational wave astronomy, high-energy cosmic rays, very high-energy photons, and neutrino astronomy are limited to this distance horizon either due to physical effects (optical depth) or instrumental sensitivity. Thus, to effectively search for an electromagnetic analog, understanding the full range of transient phenomena is essential. For instance, the electromagnetic counterpart to the gravitational wave signature of neutron star mergers is expected to be fainter and faster than that of supernovae (e.g. Metzger et al. 2010).

Our second motivation is one of pure exploration. The peak luminosity of novae ranges between  $-4$  and  $-10 \text{ mag}$ ,<sup>1</sup> whereas supernovae range between  $-15$  and  $-22 \text{ mag}$ . The large gap between the cataclysmic novae and the catastrophic supernovae has been noted by early observers. Theorists have proposed several intriguing scenarios producing transients in this “gap.” (e.g. Bildsten et al. 2007; Metzger et al. 2009; Shen et al. 2010; Moriya et al. 2010)

The Palomar Transient Factory<sup>2</sup> (PTF; see Rahmer et al. 2008; Law et al. 2009; Rau et al. 2009) was designed to undertake a systematic exploration of the transient sky in the optical bands. One of the key projects of PTF is to build a complete inventory of transients in the local Universe. PTF has a “Dynamic” cadence experiment which undertakes frequent observations of fields, optimized for inclusion of galaxies in the local Universe. A description of the design sensitivity is

given elsewhere (Kulkarni & Kasliwal 2009). Here, we report on the discovery of PTF 10fq, a transient in this “gap” between novae and supernovae.

## 2. DISCOVERY

On 2010 April 16.393 (UT dates are used throughout this paper), the Palomar Transient Factory discovered an optical transient toward Messier 99 (M99; see Figure 1). Following the PTF discovery naming sequence, this transient was dubbed PTF 10fq and reported via an ATEL (Kasliwal & Kulkarni 2010).

M99 (NGC 4254)<sup>3</sup>, an Sc galaxy, is one of the brighter spiral members of the Virgo cluster. The recession velocity of the galaxy is about  $2400 \text{ km s}^{-1}$ . Over the past fifty years, three supernovae have been discovered in this galaxy: SN 1967H (Type II?, Fairall 1972), SN 1972Q (Type II; Barbon et al. 1973),<sup>4</sup> and SN 1986I (Type II; Pennypacker et al. 1989).

At discovery, the brightness of PTF 10fq was  $R = 20.0 \pm 0.2 \text{ mag}$ . There are no previous detections in PTF data taken on and prior to April 10. If located in M99, the absolute magnitude (for an assumed distance of  $17 \text{ Mpc}$ ; Russell 2002) corresponds to  $M_R = -11.1$ . We concluded that the object could be (in decreasing order of probability) a foreground variable star, a young supernova, or a transient in the “gap.” These possibilities can be easily distinguished by spectroscopic observations.

## 3. FOLLOW-UP OBSERVATIONS

<sup>3</sup> <http://seds.org/messier/m/m099.html>

<sup>4</sup> Curiously, the reported position of SN 1972Q was only  $3.6''$  from PTF 10fq. We did a careful registration of the discovery image of SN 1972Q (Barbon et al. 1973) and PTF 10fq and find that the offset is actually  $11.0'' \text{ E}, 0.8'' \text{ S}$ .

<sup>1</sup> Unless explicitly noted, quoted magnitudes are in the  $R$  band

<sup>2</sup> <http://www.astro.caltech.edu/ptf>.

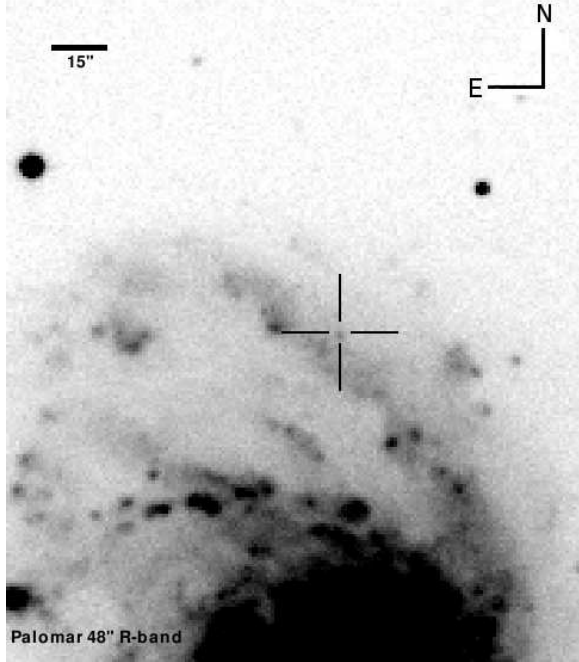


FIG. 1.— The discovery image of PTF 10fqs (obtained with the Palomar Oschin 48-inch telescope on 2010 Apr 16.393). The transient is marked by a cross and located at  $\alpha(\text{J2000}) = 12^{\text{h}}18^{\text{m}}50.16^{\text{s}}$  and  $\delta(\text{J2000}) = +14^{\circ}26'39.2''$ . With respect to the host-galaxy nucleus, the transient is offset by  $8.1''$  E and  $99.9''$  N.

### 3.1. Spectra

We triggered our Target-of-Opportunity (TOO) program on the 8-m Gemini-South telescope. On 2010 April 18.227, the Gemini Observatory staff observed PTF 10fqs with the Gemini Multi-Object Spectrograph (GMOS; Hook et al. 2004). The parameters for the observations were: R400 grating, order-blocking filter GG455\_G039, and a  $1.0''$  slit. Two 10-min integrations centered on 6700 and 6800 Å were obtained. The two observations allowed for coverage of the gap between the chips. The package `gemini gmoss` working in the `iraf` framework was used to reduce the data. The spectrum is shown in Figure 2.

The most prominent emission feature is an intermediate width ( $13 \text{ Å}$ ,  $600 \text{ km s}^{-1}$ )<sup>5</sup>  $\text{H}\alpha$  line consistent with the recession velocity of the galaxy ( $2400 \text{ km s}^{-1}$ ; see below).  $\text{H}\beta$  was not detected. From this spectrum alone, we concluded that PTF 10fqs is in M99 and the intermediate line width made it unlikely to be a supernova. PTF 10fqs appeared to be a transient in the “gap,” and we initiated extensive multi-band follow-up observations.

We continued to monitor the spectral evolution with the Marcario Low-Resolution Spectrograph (LRS; Hill et al. 1998) on the Hobby Eberly Telescope<sup>6</sup>. We used the G1 grating, with a  $2''$  slit and a GG385 order-blocking filter, providing resolution  $R = \lambda/\Delta\lambda \approx 360$  over 4200–9200 Å. Data were reduced using the `onedspec` package in the `iraf` environment, with cosmic-ray rejection via the `la_cosmic` package (van Dokkum 2001),

<sup>5</sup> The velocity quoted here is corrected for instrumental resolution and is measured as the Gaussian Full Width Half Maximum (FWHM) of the emission line.

<sup>6</sup> Director’s Discretionary Time, PI D. Fox.

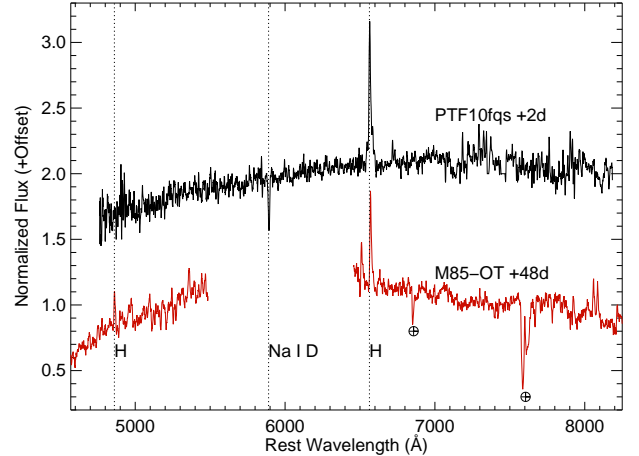


FIG. 2.— Gemini GMOS spectrum of PTF 10fqs (black) taken two days after discovery. The wavelength coverage is continuous over the range 4600 to 8800 Å. The most prominent emission feature is  $\text{H}\alpha$ . Plotted below for comparison, the spectrum of M85OT-2006-1 (red; Kulkarni et al. 2007)

TABLE 1  
LOG OF SPECTROSCOPIC OBSERVATIONS

Date (UT 2010)	MJD	Exposure	Facility	Grating/Grism
Apr 18.23	55304.23	2 × 600 s	Gemini-S/GMOS	400
Apr 21.31	55307.31	2 × 800 s	HET/LRS	360
Apr 25.29	55311.29	2 × 600 s	HET/LRS	360
Apr 30.12	55316.12	2 × 600 s	HET/LRS	360
May 3.28	55319.28	2 × 600 s	HET/LRS	360
May 15.26	55331.26	3 × 600 s	Keck I/LRIS	831
May 15.26	55331.26	1 × 2000 s	Keck I/LRIS	300
May 15.31	55331.31	3 × 650 s	Keck I/LRIS	600

and with spectrophotometric corrections applied using standard-star observations (specifically, BD332642).

On May 15, we also obtained relatively higher resolution spectroscopic observations and relatively better blue coverage with the Low Resolution Imaging Spectrograph (Oke et al. 1995) on the Keck I telescope. First, we used the 831/8200 grating centered on 7905 Å to get higher resolution spectra of the Calcium lines. On the blue side, we used the 300/5000 grism to cover Ca H+K lines. For higher resolution covering the Balmer lines, we used the 600/7500 grating (centered on 7201 Å) in conjunction with the 600/4000 grism.

The log of spectroscopic observations is given in Table 1. The spectral evolution is shown in Figure 3.

### 3.2. Optical and Near-Infrared Imaging

Observations with the robotic Palomar 60-inch telescope (Cenko et al. 2006) on April 20.4 confirmed that PTF 10fqs was rising ( $r = 19.4 \pm 0.1$  mag) and red ( $g - r = 1.0$  mag). We show the photometric evolution in *gri*-bands in Figure 4 and Table 2. On April 27.2, the light curve peaked at  $r = 18.9 \pm 0.1$  mag corresponding to  $M_r = -12.3$  (correcting for foreground Galactic extinction of  $E(B-V)=0.039$ ; Schlegel et al. 1998). Aperture photometry was done after image subtraction using a custom modification of the CPM algorithm, *mkdiff* (Gal-Yam et al. 2004). Template images for sub-

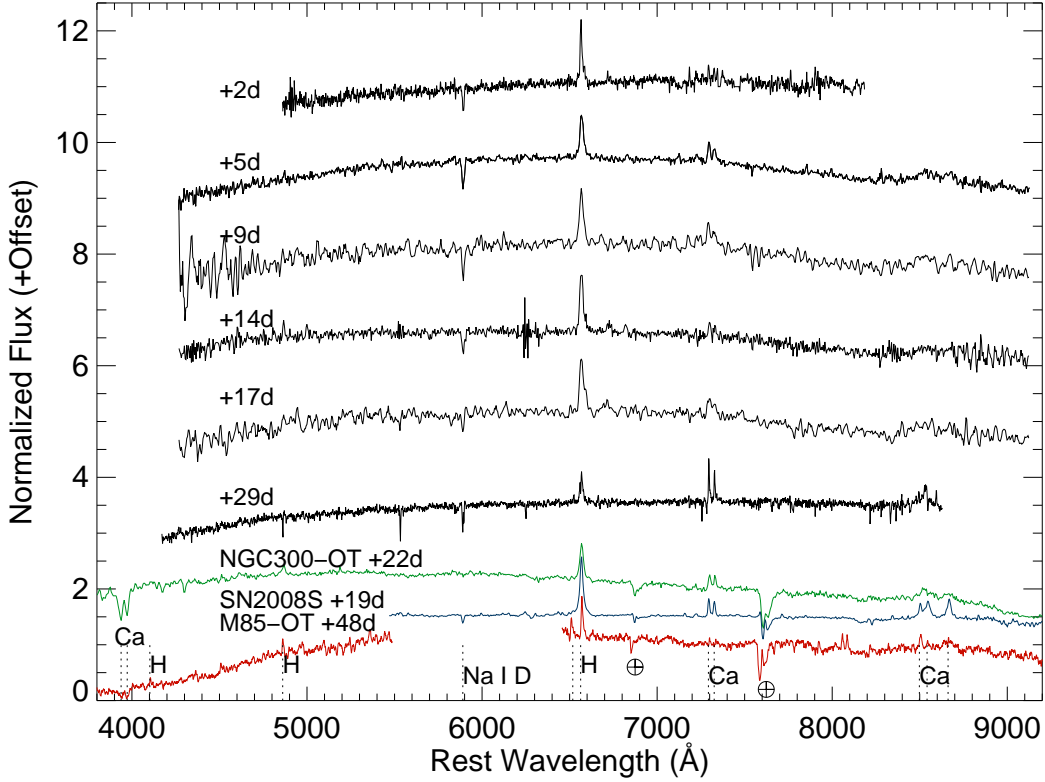


FIG. 3.— Spectra of PTF 10fq at various epochs (phase in days is defined relative to discovery epoch). Also shown are spectra of NGC 300-OT (Bond et al. 2009), M85OT2006-1 (Kulkarni et al. 2007) and SN2008S (Botticella et al. 2009). The wavelength has been corrected for the recession velocity of each galaxy ( $z = 0.0024$  for M85,  $z = 0.008$  for M99,  $z = 0.00048$  for NGC 300 and  $z = 0.00016$  for NGC 6946).

traction and reference magnitudes for zeropoint computation were taken from the Sloan Digital Sky Survey (Abazajian et al. 2009).

Near-infrared images were obtained with the Peters Automated Infrared Imaging Telescope (PAIRITEL; Bloom et al. 2006), and reduced by an automated reduction pipeline. We lack sufficiently deep template images, which are free of light from PTF 10fq, to perform reliable image subtraction. Thus, we measure the flux from the source in a small circular aperture, removing the sky with a nearby background region, and adopt a systematic error of 0.2 mag in the  $J$  and  $H$  bands and 0.3 mag in  $K_s$  band. The values reported in Table 2 have been calibrated against the 2MASS system (Cohen et al. 2003).

TABLE 2  
OPTICAL AND NEAR-INFRARED LIGHT CURVE

Date (MJD)	Filter	Mag	Facility
55295.2	<i>Mould-R</i>	>20.94	Palomar 48-in
55296.5	<i>Mould-R</i>	>19.28	Palomar 48-in
55302.4	<i>Mould-R</i>	$19.99 \pm 0.19$	Palomar 48-in
55313.2	<i>Mould-R</i>	$19.27 \pm 0.11$	Palomar 48-in
55316.3	<i>Mould-R</i>	$19.28 \pm 0.11$	Palomar 48-in
55317.3	<i>Mould-R</i>	$19.30 \pm 0.13$	Palomar 48-in
55319.2	<i>Mould-R</i>	$19.20 \pm 0.10$	Palomar 48-in
55320.2	<i>Mould-R</i>	$19.42 \pm 0.12$	Palomar 48-in
55321.3	<i>Mould-R</i>	$19.41 \pm 0.12$	Palomar 48-in
55323.2	<i>Mould-R</i>	$19.39 \pm 0.13$	Palomar 48-in
55324.2	<i>Mould-R</i>	$19.53 \pm 0.15$	Palomar 48-in
55329.2	<i>Mould-R</i>	$19.55 \pm 0.18$	Palomar 48-in
55330.2	<i>Mould-R</i>	$19.67 \pm 0.20$	Palomar 48-in

TABLE 2 — *Continued*

Date (MJD)	Filter	Mag	Facility
55331.2	<i>Mould-R</i>	$19.74 \pm 0.16$	Palomar 48-in
55332.2	<i>Mould-R</i>	$19.68 \pm 0.11$	Palomar 48-in
55333.2	<i>Mould-R</i>	$19.65 \pm 0.15$	Palomar 48-in
55336.3	<i>Mould-R</i>	$19.60 \pm 0.12$	Palomar 48-in
55337.3	<i>Mould-R</i>	$19.61 \pm 0.17$	Palomar 48-in
55343.2	<i>Mould-R</i>	$19.81 \pm 0.12$	Palomar 48-in
55346.2	<i>Mould-R</i>	$19.66 \pm 0.13$	Palomar 48-in
55347.2	<i>Mould-R</i>	$19.79 \pm 0.17$	Palomar 48-in
55348.2	<i>Mould-R</i>	$19.66 \pm 0.13$	Palomar 48-in
55349.3	<i>Mould-R</i>	$19.90 \pm 0.19$	Palomar 48-in
55351.2	<i>Mould-R</i>	$19.78 \pm 0.16$	Palomar 48-in
55352.2	<i>Mould-R</i>	$19.63 \pm 0.12$	Palomar 48-in
55353.2	<i>Mould-R</i>	$19.83 \pm 0.21$	Palomar 48-in
55355.2	<i>Mould-R</i>	$19.76 \pm 0.16$	Palomar 48-in
55356.2	<i>Mould-R</i>	$19.69 \pm 0.16$	Palomar 48-in
55361.2	<i>Mould-R</i>	$19.82 \pm 0.16$	Palomar 48-in
55362.2	<i>Mould-R</i>	$19.80 \pm 0.16$	Palomar 48-in
55363.2	<i>Mould-R</i>	$19.66 \pm 0.16$	Palomar 48-in
55364.2	<i>Mould-R</i>	$19.84 \pm 0.15$	Palomar 48-in
55368.2	<i>Mould-R</i>	$19.95 \pm 0.14$	Palomar 48-in
55371.2	<i>Mould-R</i>	$19.93 \pm 0.23$	Palomar 48-in
55372.2	<i>Mould-R</i>	$20.10 \pm 0.16$	Palomar 48-in
55373.2	<i>Mould-R</i>	$20.15 \pm 0.19$	Palomar 48-in
55375.2	<i>Mould-R</i>	$19.97 \pm 0.17$	Palomar 48-in
55377.2	<i>Mould-R</i>	$20.00 \pm 0.24$	Palomar 48-in
55379.2	<i>Mould-R</i>	$19.87 \pm 0.10$	Palomar 48-in
55304.4	<i>r</i>	$19.85 \pm 0.12$	Palomar 60-in
55306.3	<i>r</i>	$19.40 \pm 0.05$	Palomar 60-in
55310.3	<i>r</i>	$19.29 \pm 0.03$	Palomar 60-in
55312.1	<i>r</i>	$19.41 \pm 0.03$	Palomar 60-in
55313.2	<i>r</i>	$18.87 \pm 0.05$	Palomar 60-in
55314.2	<i>r</i>	$18.94 \pm 0.17$	Palomar 60-in

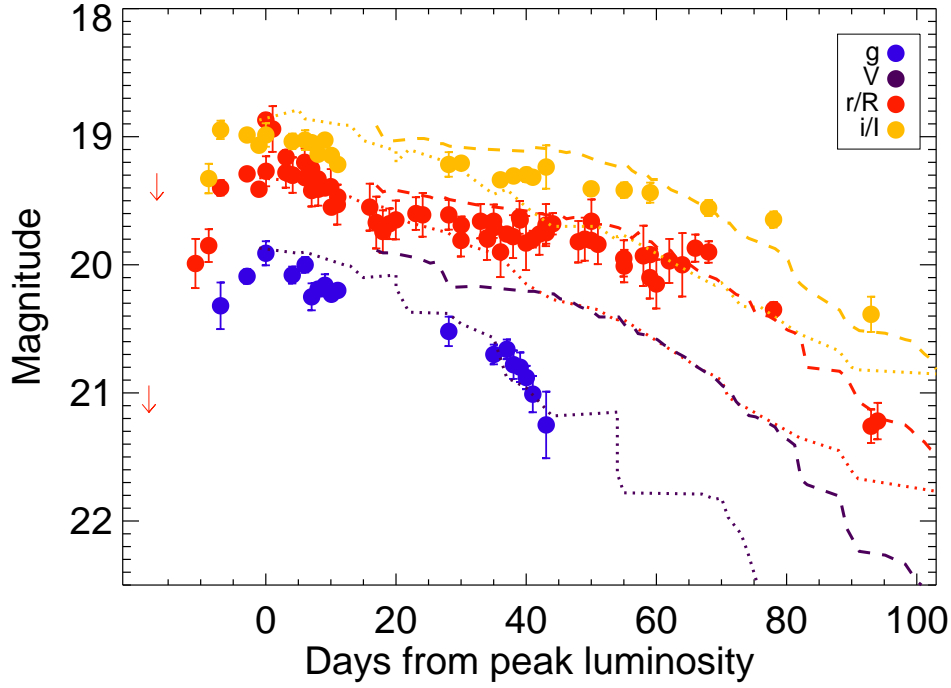


FIG. 4.— Multi-band light curve of PTF 10fq obtained with the Palomar 48-inch (squares) and Palomar 60-inch (circles) telescopes. Upper limits are denoted by downward arrows. Note that the evolution is relatively faster in the  $g$ -band compared to  $r$ -band. Also shown for comparison are the  $VRI$ -band lightcurves of SN2008S (dotted; Botticella et al. 2009) and NGC300-OT (dashed; Bond et al. 2009). The light curves are shifted vertically by a constant (+3 mag for SN2008S and +5.2 mag for NGC300-OT) such that their  $R$ -band light curves are at the same level as the  $r$ -band light curve of PTF 10fq.

TABLE 2 — *Continued*

Date (MJD)	Filter	Mag	Facility
55316.3	$r$	$19.16 \pm 0.05$	Palomar 60-in
55317.3	$r$	$19.30 \pm 0.05$	Palomar 60-in
55319.2	$r$	$19.32 \pm 0.04$	Palomar 60-in
55320.2	$r$	$19.25 \pm 0.01$	Palomar 60-in
55321.2	$r$	$19.33 \pm 0.02$	Palomar 60-in
55322.3	$r$	$19.40 \pm 0.02$	Palomar 60-in
55323.3	$r$	$19.55 \pm 0.04$	Palomar 60-in
55324.3	$r$	$19.47 \pm 0.02$	Palomar 60-in
55341.3	$r$	$19.61 \pm 0.11$	Palomar 60-in
55343.2	$r$	$19.69 \pm 0.06$	Palomar 60-in
55347.3	$r$	$19.80 \pm 0.04$	Palomar 60-in
55348.2	$r$	$19.71 \pm 0.01$	Palomar 60-in
55350.2	$r$	$19.76 \pm 0.03$	Palomar 60-in
55352.3	$r$	$19.65 \pm 0.03$	Palomar 60-in
55354.2	$r$	$19.80 \pm 0.06$	Palomar 60-in
55356.3	$r$	$19.75 \pm 0.08$	Palomar 60-in
55357.3	$r$	$19.68 \pm 0.08$	Palomar 60-in
55363.2	$r$	$19.81 \pm 0.03$	Palomar 60-in
55368.3	$r$	$20.01 \pm 0.12$	Palomar 60-in
55372.2	$r$	$19.92 \pm 0.03$	Palomar 60-in
55381.2	$r$	$19.90 \pm 0.08$	Palomar 60-in
55391.2	$r$	$20.35 \pm 0.05$	Palomar 60-in
55406.2	$r$	$21.26 \pm 0.13$	Palomar 60-in
55407.2	$r$	$21.22 \pm 0.14$	Palomar 60-in
55306.3	$g$	$20.32 \pm 0.18$	Palomar 60-in
55310.3	$g$	$20.09 \pm 0.05$	Palomar 60-in
55313.2	$g$	$19.91 \pm 0.09$	Palomar 60-in
55317.3	$g$	$20.08 \pm 0.06$	Palomar 60-in
55319.2	$g$	$20.00 \pm 0.06$	Palomar 60-in
55320.2	$g$	$20.25 \pm 0.10$	Palomar 60-in
55321.2	$g$	$20.19 \pm 0.03$	Palomar 60-in
55322.3	$g$	$20.16 \pm 0.08$	Palomar 60-in
55323.3	$g$	$20.23 \pm 0.04$	Palomar 60-in
55324.3	$g$	$20.20 \pm 0.02$	Palomar 60-in
55341.3	$g$	$20.52 \pm 0.11$	Palomar 60-in

TABLE 2 — *Continued*

Date (MJD)	Filter	Mag	Facility
55348.2	$g$	$20.70 \pm 0.07$	Palomar 60-in
55350.2	$g$	$20.66 \pm 0.07$	Palomar 60-in
55351.3	$g$	$20.78 \pm 0.11$	Palomar 60-in
55352.3	$g$	$20.80 \pm 0.11$	Palomar 60-in
55353.2	$g$	$20.88 \pm 0.09$	Palomar 60-in
55354.2	$g$	$21.01 \pm 0.14$	Palomar 60-in
55356.3	$g$	$21.25 \pm 0.25$	Palomar 60-in
55304.4	$i$	$19.32 \pm 0.11$	Palomar 60-in
55306.3	$i$	$18.94 \pm 0.07$	Palomar 60-in
55310.3	$i$	$18.98 \pm 0.03$	Palomar 60-in
55312.2	$i$	$19.06 \pm 0.04$	Palomar 60-in
55313.2	$i$	$18.98 \pm 0.09$	Palomar 60-in
55317.3	$i$	$19.03 \pm 0.06$	Palomar 60-in
55319.2	$i$	$19.02 \pm 0.07$	Palomar 60-in
55320.2	$i$	$19.04 \pm 0.03$	Palomar 60-in
55321.2	$i$	$19.13 \pm 0.03$	Palomar 60-in
55322.3	$i$	$19.02 \pm 0.04$	Palomar 60-in
55323.3	$i$	$19.14 \pm 0.03$	Palomar 60-in
55324.2	$i$	$19.21 \pm 0.04$	Palomar 60-in
55341.3	$i$	$19.21 \pm 0.09$	Palomar 60-in
55343.2	$i$	$19.20 \pm 0.02$	Palomar 60-in
55349.2	$i$	$19.33 \pm 0.02$	Palomar 60-in
55351.3	$i$	$19.30 \pm 0.03$	Palomar 60-in
55353.2	$i$	$19.29 \pm 0.05$	Palomar 60-in
55354.2	$i$	$19.31 \pm 0.03$	Palomar 60-in
55356.3	$i$	$19.23 \pm 0.16$	Palomar 60-in
55363.2	$i$	$19.40 \pm 0.05$	Palomar 60-in
55368.3	$i$	$19.41 \pm 0.05$	Palomar 60-in
55372.2	$i$	$19.43 \pm 0.07$	Palomar 60-in
55381.2	$i$	$19.55 \pm 0.06$	Palomar 60-in
55391.2	$i$	$19.64 \pm 0.06$	Palomar 60-in
55406.2	$i$	$20.38 \pm 0.13$	Palomar 60-in
55307.2	$J$	$18.14 \pm 0.29$	PAIRITEL
55315.2	$J$	$18.37 \pm 0.39$	PAIRITEL
55317.2	$J$	$17.89 \pm 0.30$	PAIRITEL

TABLE 2 — *Continued*

Date (MJD)	Filter	Mag	Facility
55319.2	<i>J</i>	17.86 ± 0.26	PAIRITEL
55321.2	<i>J</i>	17.94 ± 0.24	PAIRITEL
55322.2	<i>J</i>	18.38 ± 0.25	PAIRITEL
55324.2	<i>J</i>	17.88 ± 0.21	PAIRITEL
55325.2	<i>J</i>	17.55 ± 0.32	PAIRITEL
55327.2	<i>J</i>	17.86 ± 0.25	PAIRITEL
55331.2	<i>J</i>	17.25 ± 0.18	PAIRITEL
55333.2	<i>J</i>	17.82 ± 0.24	PAIRITEL
55369.2	<i>J</i>	17.78 ± 0.31	PAIRITEL
55307.2	<i>H</i>	17.35 ± 0.21	PAIRITEL
55315.2	<i>H</i>	17.37 ± 0.27	PAIRITEL
55317.2	<i>H</i>	17.14 ± 0.22	PAIRITEL
55319.2	<i>H</i>	16.81 ± 0.27	PAIRITEL
55321.2	<i>H</i>	17.75 ± 0.18	PAIRITEL
55322.2	<i>H</i>	17.25 ± 0.16	PAIRITEL
55324.2	<i>H</i>	17.22 ± 0.20	PAIRITEL
55325.2	<i>H</i>	17.19 ± 0.30	PAIRITEL
55327.2	<i>H</i>	17.02 ± 0.20	PAIRITEL
55331.2	<i>H</i>	16.97 ± 0.32	PAIRITEL
55333.2	<i>H</i>	17.07 ± 0.29	PAIRITEL
55369.2	<i>H</i>	17.22 ± 0.22	PAIRITEL
55307.2	<i>K</i>	16.17 ± 0.18	PAIRITEL
55315.2	<i>K</i>	16.56 ± 0.31	PAIRITEL
55317.2	<i>K</i>	16.84 ± 0.19	PAIRITEL
55319.2	<i>K</i>	16.90 ± 0.25	PAIRITEL
55321.2	<i>K</i>	16.84 ± 0.40	PAIRITEL
55322.2	<i>K</i>	16.69 ± 0.21	PAIRITEL
55324.2	<i>K</i>	16.29 ± 0.15	PAIRITEL
55325.2	<i>K</i>	16.73 ± 0.18	PAIRITEL
55327.2	<i>K</i>	16.65 ± 0.22	PAIRITEL
55331.2	<i>K</i>	>15.80	PAIRITEL
55333.2	<i>K</i>	>16.60	PAIRITEL
55369.2	<i>K</i>	>16.36	PAIRITEL

### 3.3. Radio Observations

We observed PTF10fqz with the EVLA on April 20.19–20.26 at central frequencies of 4.96 GHz and 8.46 GHz. We added together two adjacent 128 MHz subbands with full polarization to maximize continuum sensitivity. Amplitude and bandpass calibration was achieved using a single observation of J1331+3030, and phase calibration was carried out every 10 min by switching between the target field and the point source J1239+0730. The visibility data were calibrated and imaged in the *AIPS* package following standard practice.

A radio point source was not detected at the position of the transient. After removing extended emission from the host galaxy, the  $3\sigma$  limits for a point source are 93  $\mu$ Jy and 63  $\mu$ Jy at 4.96 GHz and 8.46 GHz, respectively. At the distance of M99, this corresponds to  $L_\nu < 2.1 \times 10^{25}$  erg s $^{-1}$  Hz $^{-1}$ . Comparing with the compilation in Chevalier et al. (2006), this upper limit is at the level of the faintest Type II-P (SN 2004dj; Beswick et al. 2005) and Type Ic (SN 2002ap; Berger et al. 2002) supernovae. As noted by Berger et al. (2009), the nearby NGC300-OT was also not detected in the radio to deeper luminosity limits.

### 3.4. Ultraviolet Observations

We observed PTF10fqz with *GALEX* (Martin et al. 2005) on two consecutive orbits starting at 2010 April 24.387 (total exposure of 2846 s). All images were reduced and coadded using the standard *GALEX* pipeline and calibration (Morrissey et al. 2007).

To create a reference image, we coadded 22 images of M99 prior to 2005 April 2 (total exposure of 18571 s).

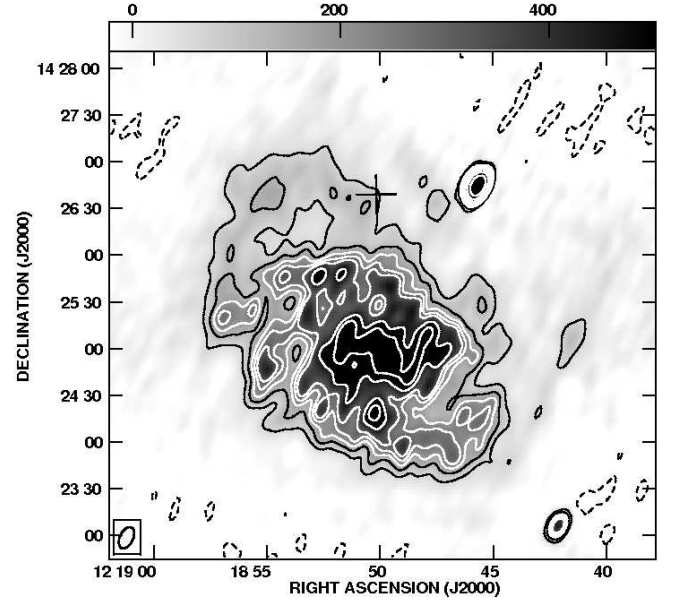


FIG. 5.— Observation of PTF10fqz (denoted by a plus sign) with the EVLA at 4.96 GHz, just four days after discovery. The gray-scale range is  $-40$  to  $1000 \mu$ Jy per beam and the size of the synthesized beam is shown at the bottom-left corner.

Next, we subtracted the reference image from observations of PTF10fqz (see Figure 6). No source is detected. We find a  $3\sigma$  upper limit of NUV 22.7 AB mag in an aperture consistent with a *GALEX* point source ( $7.5'' \times 7.5''$ ).

To constrain the pre-explosion counterpart, we measured the limiting magnitude at the position of PTF10fqz in the coadded reference image. The faintest detected object consistent with being a point source within the galaxy had NUV = 20.1 AB mag. The  $3\sigma$  limit based on measuring the sky root-mean square (rms) is NUV > 21.8 AB mag.

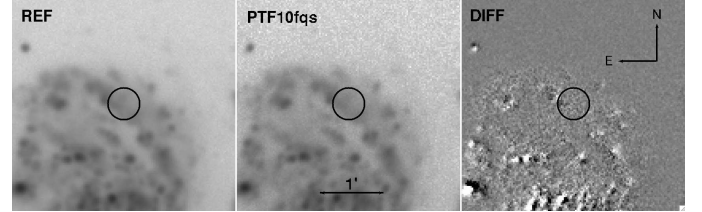


FIG. 6.— Observation of PTF10fqz with *GALEX*. Reference data are taken from 22 images between 28 March 2005 and 2 April 2005 (left panel). Observations of PTF10fqz were taken on 24 April 2010 (center panel). No source is detected in the difference image (right panel).

### 3.5. X-ray Observations

We observed PTF10fqz with *Swift*/XRT on April 20.466 for 2507.3 s and April 22.024 for 2623.5 s. No source is detected to a  $3\sigma$  limiting count rate (assuming an  $18''$  radius) of  $4.6 \times 10^{-4}$  counts s $^{-1}$ . Assuming a power-law model with a photon index of two, this corresponds to a flux limit of  $1.6 \times 10^{-14}$  erg cm $^{-2}$  s $^{-1}$ .

## 4. ARCHIVAL DATA

### 4.1. Hubble Space Telescope (HST)



TABLE 3  
PTF 10fqs BROADBAND MEASUREMENTS

Date (UT 2010)	MJD	Filter	Magnitude/Flux	$\nu$ (Hz)	$\nu F_\nu$ (erg cm <sup>-2</sup> s <sup>-1</sup> )	Facility
Apr 20.23	55306.23	4.96 GHz	<93 $\mu$ Jy	$4.960 \times 10^9$	$4.613 \times 10^{-18}$	EVLA
Apr 20.23	55306.23	8.46 GHz	<63 $\mu$ Jy	$8.460 \times 10^9$	$5.330 \times 10^{-18}$	EVLA
Apr 20.466	55306.466	0.3–10 keV	< $4.6 \times 10^{-4}$ cps	$4.200 \times 10^{17}$	$2.864 \times 10^{-15}$	<i>Swift</i> /XRT
Apr 24.646	55310.646	NUV (AB)	>22.7 mag	$1.295 \times 10^{15}$	$3.885 \times 10^{-14}$	<i>GALEX</i>

TABLE 4  
PROGENITOR CONSTRAINTS FOR PTF 10fqs

Date	Filter	Magnitude/Flux	Facility
2005	NUV (AB)	>21.8 mag	<i>GALEX</i>
2009	F336W (Vega <i>U</i> )	>26 mag	<i>HST</i> /WFPC2
2009	F814W (Vega <i>I</i> )	>26.9 mag	<i>HST</i> /WFPC2
2004	3.6 $\mu$ m	<5.3 $\mu$ Jy	<i>Spitzer</i> /IRAC
2004	4.5 $\mu$ m	<3.5 $\mu$ Jy	<i>Spitzer</i> /IRAC
2004	5.8 $\mu$ m	<51 $\mu$ Jy	<i>Spitzer</i> /IRAC
2004	8.0 $\mu$ m	<344 $\mu$ Jy	<i>Spitzer</i> /IRAC
2004	23.68 $\mu$ m	<240 $\mu$ Jy	<i>Spitzer</i> /MIPS

A query to the Hubble Legacy archive returned *HST* images of M99 in the F606W (2001), F336W (2009), and F814W (2009) filters. We multidrizzled this data (PI Regan, Proposal ID 11966) and registered our Gemini/GMOS acquisition image with the *HST*/WFPC2 images. Unfortunately, PTF 10fqs is just off the edge of the chip for the F606W filter image.

The total  $1\sigma$  registration error, added in quadrature, was 0.59 pixels. There sources of error are as follows: centroiding error (0.17 in *x*, 0.30 in *y*), registration error between the Gemini image and *HST*/F814W image (0.19 in *x*, 0.44 in *y*) and registration error between *HST*/F814W image and *HST*/F336W image (0.04 in *x*, 0.02 in *y*). Hence, in Figure 7 we plot a  $5\sigma$  radius of 3 pixels or 0.27".

No source is detected at the location of PTF 10fqs. To estimate the limiting magnitude, we ran *sextractor* and performed photometry following Holtzman et al. (1995). We find  $3\sigma$  limiting Vega magnitudes of  $I > 26.9$  and  $U > 26$  in the 1800s and 6600s exposures respectively.

#### 4.2. *Spitzer Space Telescope*

M99 was part of the sample of the SIRTf Nearby Galaxies Survey (SINGS) galaxies (Kennicutt et al. 2003). This program undertook IRAC and MIPS imaging in 2004–2005. No point source is detected at the location of PTF 10fqs (see Figure 8). We downloaded IRAC images from the final data release of SINGS and MIPS images from the standard *Spitzer* pipeline. Computed upper limits (see Table 4) assume a 2-pixel aperture radius and sky-rms based on a  $20 \times 20$  pixel box at the location.

#### 4.3. *Katzman Automatic Imaging Telescope*

The 0.76 m Katzman Automatic Imaging Telescope (KAIT<sup>7</sup>; Li et al. 2000; Filippenko et al. 2001) had extensively imaged M99 in the past decade — 113 images in

TABLE 5  
HISTORICAL OPTICAL OBSERVATIONS

Date Range (UT)	Exposure (seconds)	Limiting Mag ( <i>R</i> band)	Facility
1998-12-27 – 1999-06-01	680.0	> 20.4	KAIT
1999-11-26 – 2000-06-07	567.0	> 20.4	KAIT
2001-04-11 – 2001-06-07	192.0	> 20.1	KAIT
2002-01-14 – 2002-06-08	486.0	> 20.4	KAIT
2003-01-15 – 2003-06-04	318.0	> 20.4	KAIT
2004-01-29 – 2004-06-16	392.0	> 20.3	KAIT
2004-12-25 – 2005-06-01	110.0	> 20.3	KAIT
2006-01-12 – 2006-05-18	665.7	> 22.2	DeepSky
2006-03-24 – 2006-05-18	78.0	> 20.4	KAIT
2007-01-04 – 2007-05-06	1749.9	> 22.4	DeepSky
2007-01-13 – 2007-06-04	178.0	> 20.4	KAIT
2007-12-22 – 2008-06-16	332.0	> 20.4	KAIT
2008-05-18 – 2008-05-18	241.2	> 20.7	DeepSky
2009-03-28 – 2009-04-27	64.0	> 20.3	KAIT
2010-02-11 – 2010-03-22	32.0	> 20.0	KAIT

NOTE. — All images in a season were stacked.

the period 1999–2010. We stacked the images in each season and find no point source at the location of PTF 10fqs. Limiting magnitudes for each season are summarized in Table 5.

#### 4.4. *DeepSky imaging*

DeepSky<sup>8</sup> (Nugent 2009) also has imaging at the position of this field over the interval 2006–2008. No point source is detected in a yearly sum of these images (see Table 5).

### 5. ANALYSIS

#### 5.1. *SED*

We fit a blackbody spectrum to the optical and near-infrared fluxes of PTF10fqs without taking into account any local extinction. The best fit gives a lower limit on the temperature of  $\sim 3900$  K.

#### 5.2. *Spectral Modelling*

We combined the four spectra obtained with HET (between +5 days and +17 days). The most prominent (narrow) features in the spectra of PTF 10fqs are H $\alpha$ , [Ca II], the Ca II near-IR triplet, Na I D, and H $\beta$ . The measured line fluxes and equivalent widths are summarized in Table 6. The H $\alpha$  FWHM is  $\approx 930$  km s<sup>-1</sup> (taking into account the instrumental resolution).

The Ca II near-IR triplet is of particular interest. The HET spectra appear to show a flux excess longward of 8300 Å beyond that expected from a simple, low-order

<sup>7</sup> <http://astro.berkeley.edu/~bait/kait.html>.

<sup>8</sup> <http://supernova.lbl.gov/~nugent/deepsky.html>.

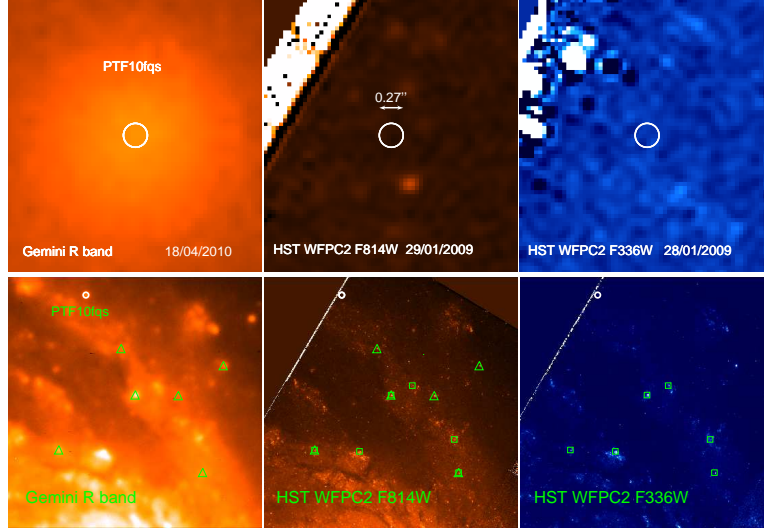


FIG. 7.— HST/F814W and HST/F336W observations from 2009. *Top panel:* Zoomed-in view ( $2.8'' \times 2.6''$ ) to show the absence of a pre-explosion counterpart. This rules out red supergiants fainter than  $M_V = -3$  mag and blue supergiants fainter than  $M_V = -4.3$  mag. *Bottom panel:* Zoomed-out view ( $81.2'' \times 82.1''$ ) to show registration stars. Stars used to register the Gemini/R-band image with the HST/F814W image are denoted by triangles. Stars used to register the HST/F814W image with the HST/F336W are denoted by squares.

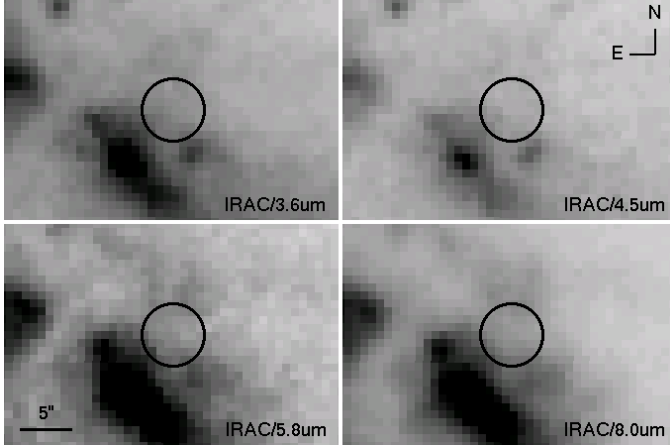


FIG. 8.— Pre-explosion observations with *Spitzer*/IRAC. No source is found to be consistent with PTF 10fq.

TABLE 6  
PTF 10FQS SPECTRUM PROPERTIES

Line	Obs $\lambda$ ( $\text{\AA}$ )	Flux ( $\text{erg cm}^{-2} \text{s}^{-1}$ )	Eq. Width $\text{\AA}$
H $\alpha$	6621.2	$1.0 \times 10^{-15}$	-19.9
H $\beta$	4907.3	$1.3 \times 10^{-16}$	-3.7
Na I D	5939.0	$-3.1 \times 10^{-16}$	6.4
[Ca II]	7355.8	$2.9 \times 10^{-16}$	-6.1
[Ca II]	7387.2	$1.8 \times 10^{-16}$	-3.7

NOTE. — Above line fluxes are measured on combined HET spectra (phase between +5 days and +17 days)

polynomial fit to the continuum. Together with a possible broad flux deficit near  $8300 \text{\AA}$ , the overall effect suggests a P-Cygni profile. If we fit three Gaussians, the Ca II near-IR triplet features are broader than the [Ca II] doublet, and quite likely even broader than the narrow component of the H $\alpha$  profile. There is a surplus of flux at

$8600 \text{\AA}$ , which falls right between the  $8498.02, 8542.09 \text{\AA}$  pair and the more isolated  $8662.14 \text{\AA}$  line, such as one would expect from an underlying broad feature.

We test this hypothesis further with SYNOW (Jeffery & Branch 1990) modelling. We do not get a good fit to the overall shape of the spectrum with an extinguished blackbody of any temperature (assuming standard dust). To fit the red end of the spectrum, we need high temperature and extinction (consistent with the strong Na I D absorption). We find that in addition to narrow emission from Ca II IR, there is also a likely underlying broad component (see Figure 9). The width (FWHM) of this feature is  $\approx 10,000 \text{ km s}^{-1}$ .

A caveat to this interpretation is that a similar broad feature is not seen in the H $\alpha$  profile. However, as noted below (§6.2), reinspection of the spectra of related transients shows possible evidence of a similar broad feature. Thus, we cautiously accept the interpretation that in addition to the low-velocity outflow seen in H $\alpha$ , there is a higher velocity outflow in this explosion.

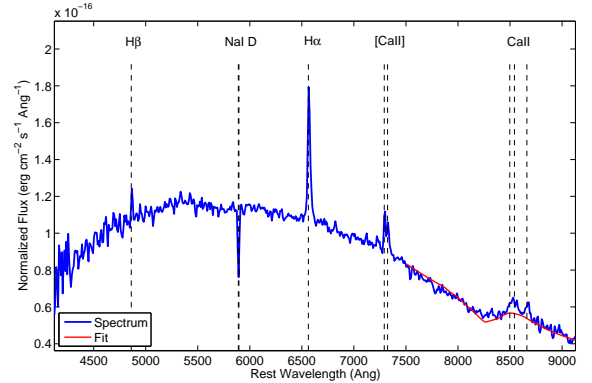


FIG. 9.— SYNOW fit to summed HET spectra of PTF10fq. Note the broad, possibly P Cygni, feature under the Ca II near-IR triplet.



## 6. WHAT IS PTF 10FQS?

In a nutshell, PTF 10fqs is a red transient with a peak luminosity of  $M_r = -12.3$  and a spectrum dominated by  $H\alpha$ ,  $[Ca II]$ , and  $Ca II$  emission. The width of the  $H\alpha$  line is  $\approx 930 \text{ km s}^{-1}$ , and there is some evidence for a  $\approx 10,000 \text{ km s}^{-1}$  broad  $Ca II$  IR feature.

The peak absolute magnitude and the  $H\alpha$  line width of PTF 10fqs are similar to those seen in M85OT2006-1 (hereafter, M85-OT; Kulkarni et al. 2007), SN 2008S (Prieto et al. 2008; Smith et al. 2009), and NGC 300-OT (Bond et al. 2009; Berger et al. 2009). However, there are some differences amongst these four sources. Thus, to aid a better classification, we review the similarities and differences between these four sources.

### 6.1. The Light Curve

The light curves of all four transients (PTF 10fqs, SN 2008S, NGC 300-OT, and M85-OT) were red and evolved slowly for the first couple of months. PTF 10fqs had a well-sampled rise (Figure 4) — it rose by 1.1 mag in  $r$ -band in 10.8 days. After maximum, PTF 10fqs declined slowly in  $r$ -band by 1 mag in 68 days. Subsequently, it evolved more rapidly, declining by the next 1.3 mag in 16 days. PTF 10fqs had  $g - r = 1.0$  at peak and declined relatively faster in  $g$ -band (1 mag in 40 days) than  $r$ -band. In comparison, SN 2008S declined by 1 mag in 51 days in  $R$ -band and 44 days in  $V$ -band. The epoch of maximum light is uncertain for NGC 300-OT due to lack of observations and is constrained to be anywhere between April 24 and May 15, 2008 (Bond et al. 2009). If we assume it to be April 27, the evolution in  $R$ -band and  $I$ -band are similar to that for PTF 10fqs (Figure 4).

### 6.2. The Spectrum

The spectral evolution of SN 2008S (Botticella et al. 2009) and NGC 300-OT (Berger et al. 2009) were very well studied as they were in very nearby galaxies. We took this opportunity to reanalyze the spectrum of M85-OT reported by (Kulkarni et al. 2007)<sup>9</sup>.

Armed thus, we compare and contrast the spectral features of these four transients (see Figure 10).

- The  $H\alpha$  profile of SN 2008S showed a narrow component (unshocked circumstellar material [CSM];  $\approx 250 \text{ km s}^{-1}$ ), an intermediate component (shocked material between the ejecta and the CSM;  $\approx 1000 \text{ km s}^{-1}$ ), and a broad component (underlying ejecta emission;  $\approx 3000 \text{ km s}^{-1}$ ). NGC 300-OT exhibited narrow ( $560 \text{ km s}^{-1}$ ) and intermediate-width components ( $1100 \text{ km s}^{-1}$ ). M85-OT only had a narrow component ( $350 \text{ km s}^{-1}$ ). PTF 10fqs shows an intermediate-width component ( $930 \text{ km s}^{-1}$ ) in the  $H\alpha$  emission line.
- SN 2008S had an  $H\alpha/H\beta$  ratio that evolved from 4 to 10. NGC 300-OT had a ratio of 6, while M85-OT showed a ratio of 3.5. PTF 10fqs has a

<sup>9</sup> In addition to the features mentioned by Kulkarni et al. 2007, we can securely identify  $Ca II$  H&K and see evidence of  $[Ca II]$  and the  $Ca II$  near-IR triplet. Furthermore, we can identify the lines previously marked “unidentified”:  $4115 \text{ \AA}$  is  $H\gamma$ ,  $6428 \text{ \AA}$  is likely Fe II (multiplet 74),  $6527 \text{ \AA}$  is likely Fe II (multiplets 40 and 92).

ratio of 6.5. All events show flux ratios higher than 3.1 (the expectation from Case B recombination). This may be evidence for collisional excitation (Drake & Ulrich 1980).

- PTF 10fqs, NGC 300-OT and SN 2008S exhibit three calcium features:  $Ca II$  H&K in absorption,  $[Ca II]$  and  $Ca II$  near-IR triplet in emission. A reanalysis of M85-OT shows  $Ca II$  H&K, as well as lower signal-to-noise ratio detections of both  $[Ca II]$  and  $Ca II$  IR. Smith et al. 2009 show a similarity between the spectra of SN 2008S and a Galactic hypergiant (IRC+10420) and suggest that strong  $[Ca II]$  is due to destruction of dust grains.
- As noted earlier (see also Figure 9), there is evidence for a broad feature around  $8600 \text{ \AA}$  in the spectrum of PTF 10fqs. Motivated by this finding, we reinspected the spectra of previous transients and find that a similar broad feature may also be present in the spectra of M85-OT and NGC 300-OT.
- Narrow Fe II lines are visible in NGC 300-OT and SN 2008S. Reanalysis of M85-OT spectra possibly shows Fe II(74) and Fe II (40, 92).
- For SN 2008S, Na I D evolves from strong absorption at early times to emission at very late times. This suggests a very dense CSM. O I  $\lambda 7774$  is also in emission at late times. For NGC 300-OT, Na I D has a much lower equivalent width at early times, but it also evolves from absorption to emission. Neither Na I D nor O I are seen in M85-OT, but there is possibly K I in emission. PTF 10fqs has an equivalent width of Na I D of 6.4, higher than SN 2008S (2.3–4.4) and NGC 300-OT (1.0–2.1). The equivalent width of Na I D is too high to apply a standard correlation to estimate extinction.

### 6.3. The Pre-Explosion Counterpart

We plot the upper limits on the pre-explosion counterpart for PTF 10fqs in Figure 11. The most constraining limits are in the optical. Following the Geneva stellar evolution tracks (Lejeune & Schaerer 2001) for unshrouded stars, the luminosity limit of  $M_I > -4.3$  corresponds to a progenitor mass  $< 4 M_\odot$ . If there was extinction of, say 1.5 mag, this would change the limit to  $< 7 M_\odot$ . None of SN 2008S, NGC 300-OT, M85-OT, and PTF 10fqs have an optical counterpart in deep, pre-explosion optical images. The limits in all cases are deep enough to at least rule out red supergiants and blue supergiants.

For both SN 2008S and NGC 300-OT, an extremely red and luminous mid-infrared pre-explosion counterpart is seen (Prieto et al. 2008; Thompson et al. 2009). Recently, Khan et al. (2010) show that such progenitors are as rare as 1 per galaxy (and possibly associated with a very short-lived phase of many massive stars). Thus, both of these transients can be reasonably associated with massive stars. Unfortunately, the large distance to M85 and M99 means that the pre-explosion *Spitzer* limits on M85-OT and PTF 10fqs are not deep enough by a factor of few to constrain their progenitors to similar depths (see Figure 12).

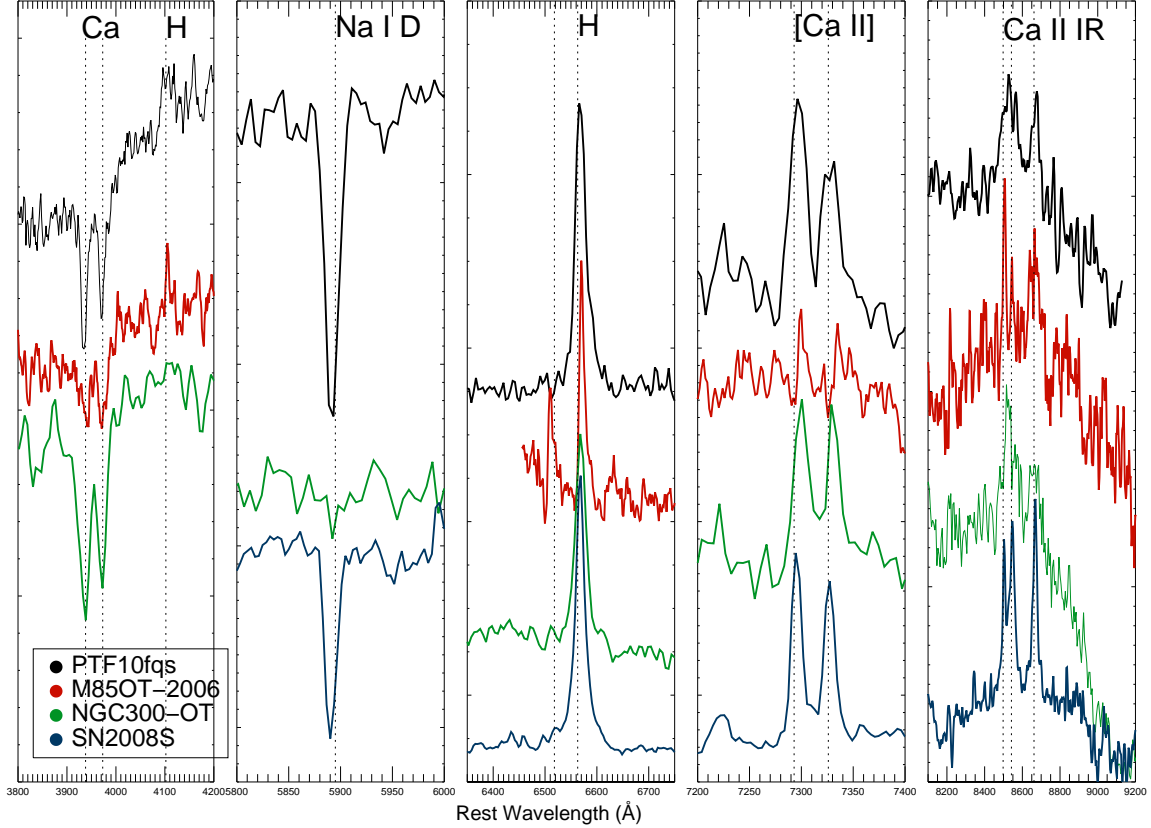


FIG. 10.— Comparison of specific lines in spectra of PTF 10fqs (black), M85-OT (red; Kulkarni et al. 2007), SN2008s (blue; Botticella et al. 2009) and NGC 300-OT (green; Bond et al. 2009). *From left to right:* Panel 1 shows Ca II H&K in all three transients. Panel 2 shows the extreme Na I D absorption in PTF 10fqs. Panel 3 shows the similar H $\alpha$  widths in all three transients. Note the presence of Fe II in M85-OT. Panel 4 shows narrow [Ca II] in all three transients. Panel 5 shows Ca II near-IR triplet. Note that in addition to the narrow lines, there is possibly an underlying broad feature.

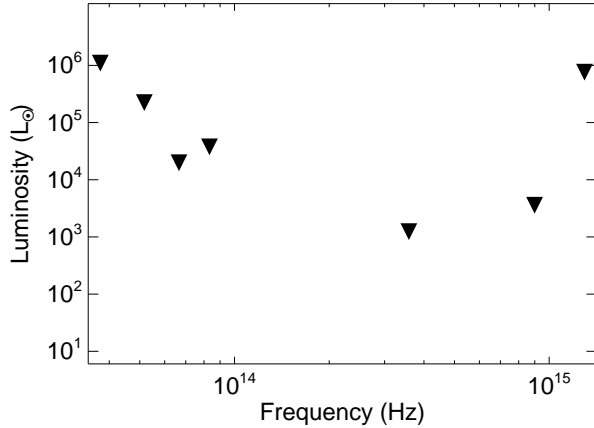


FIG. 11.— Spectral energy distribution (mid-IR to UV) constraints on the pre-explosion counterpart of PTF 10fqs. Upper limits are denoted by downward arrows.

#### 6.4. The Large-Scale Environment

M85-OT is located in the lenticular galaxy M85 (also in the Virgo cluster). Fortunately, this galaxy was observed with *HST* for the ACS Virgo Cluster Survey as well as for a GO program. The transient is not associated with any star-forming region and the absolute mag-

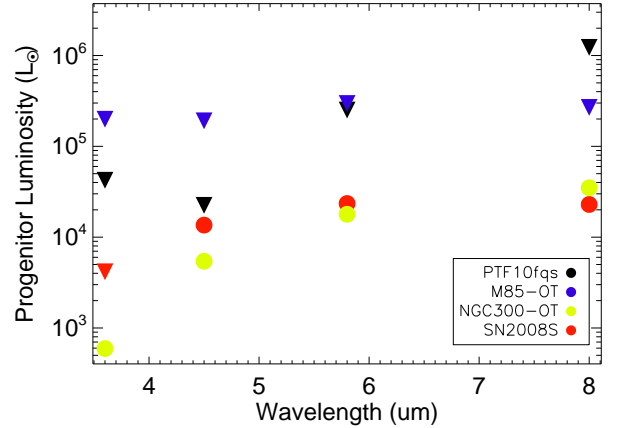


FIG. 12.— Pre-explosion detections (circles) or upper limits (downward triangles) from *Spitzer* for PTF 10fqs, SN2008S, NGC 300-OT, and M85-OT. The non-detection of a progenitor for PTF 10fqs and M85-OT does not rule out a progenitor of luminosity comparable to that detected for NGC 300-OT and SN2008S.

nitude of the progenitor is fainter than  $M_g \approx -4$  ( $< 7 M_\odot$  not correcting for extinction; Ofek et al. 2008). Thus, a massive-star origin is quite unlikely.

In contrast, SN 2008S, NGC 300-OT, and PTF 10fqs occurred in star-forming galaxies. It may be worth not-

ing here that three supernovae (all of the core-collapse variety) have previously been discovered in the host galaxy of PTF 10fq. It is perhaps of some significance that eight supernovae (six core-collapse, two unclassified) were discovered in NGC 6946 in addition to SN 2008S. Only one supernova (of Type Ia) has been discovered in NGC 300. Small-number statistics and discovery bias (incompleteness from variety of different searches) notwithstanding, we make the suggestion that galaxies with a high supernova rate preferentially produce luminous red novae. If this suggestion is correct, then it would be worth the effort to systematically maintain close vigilance on the nearest galaxies having large supernova rates.

Kulkarni et al. 2007 suggested that V838 Mon, V4332 Sgr and M31 RV may also be luminous, red novae. We note here that the two Galactic sources are located in star-forming regions. Specifically, V838 Mon is in a young (25 Myr) star cluster and may even have a B3 companion (Afşar & Bond 2007). V4332 Sgr (Martini et al. 1999) is located towards the inner Galaxy (in Sagittarius). On the other hand, M31 RV is located in the bulge of M31. *HST* observations (undertaken with WFPC2 in parallel mode) taken about a decade ago show that the immediate environs of M31-RV are typical bulge-population stars (Bond & Siegel 2006). No unusual remnant star is seen at the astrometric position of M31 RV, nor any evidence of a light echo (consistent with the absence of dense circumstellar or interstellar gas that is essential to form echoes). Separately, there is no evidence for any luminous outbursts in this area in the period 1942–1993 (Boschi & Munari 2004). Thus, M31 RV appears to have been a cataclysmic event in the bulge of M31.

## 7. CONCLUSION

PTF 10fq is the fourth member of a class of extragalactic transients<sup>10</sup> which possess a peak luminosity between that of novae and supernovae, and have spectral and photometric evolution that bear no resemblance to either supernovae or novae. The other members of this class are M85-OT, NGC 300-OT, SN 2008S.

NGC 300-OT and SN 2008S are remarkable for their very bright mid-infrared progenitors. Though sensitive pre-explosion observations of M85-OT and PTF 10fq do exist, the large distance to the Virgo Cluster (17 Mpc) relative to that of NGC 300 (1.9 Mpc) and NGC 6946 (5.7 Mpc) results in weak constraints on the luminosity of any pre-explosion star. PTF 10fq, NGC 300-OT, and SN 2008S occurred in star-forming regions whereas M85-OT was in the bulge. *Prima facie*, this group of explosive events can be divided into a disk and a bulge group.

The discovery of PTF 10fq in itself cannot address whether the two groups of luminous, red novae are one and the same. The proposed models to explain this group are diverse: electron capture within an extreme asymptotic giant branch (AGB) star, common-envelope phase (stellar merger), inspiral of a giant planet into the envelope of an aging parent star, a most peculiar nova, and a most peculiar supernova.

The possible evidence of the broad feature centered around the Ca II near-IR triplet with an inferred veloc-

ity spread of  $10,000 \text{ km s}^{-1}$  may be an important clue. It would mean that these events possess both a low- and a high-velocity outflow. By comparison with other astronomical sources, one can envisage a high-velocity polar outflow and a slower equatorial outflow (but with a larger mass). To this end, continued sensitive spectroscopy of PTF 10fq (and of course other such future events) would be very valuable.

The “Transients in the Local Universe” key project of the Palomar Transient Factory is designed to systematically unveil events in the gap between novae and supernovae. It surveys  $\approx 20,000$  nearby galaxies ( $d < 200 \text{ Mpc}$ ) yearly at 1-day cadence and a depth of  $R < 21 \text{ mag}$ . (If the maximum luminosity of this class is  $-14 \text{ mag}$ , then we would be sensitive to events out to  $100 \text{ Mpc}$ .) Furthermore, *Spitzer* has a growing archive of deep images of nearby galaxies (e.g., SINGS, Kennicutt et al. 2003; LVL, Dale et al. 2009, and S4G, Sheth et al. 2010), and *WISE* (Wright et al. 2010) has an ongoing all-sky survey in the mid-IR. This will allow us to probe deeper in search of the pre-explosion counterpart and possibly present a new channel for discovery of luminous red novae. The discovery of PTF 10fq is only the harbinger of the uncovering of a large sample of such transients to unveil the nature of this new class of explosions.

## Acknowledgments.

M.M.K. thanks the Gordon and Betty Moore Foundation for a Hale Fellowship in support of graduate study. The Weizmann Institute PTF participation is supported in part by the Israel Science Foundation via grants to AGY. The Weizmann-Caltech collaborative PTF effort is supported by the US-Israel Binational Science Foundation. AGY and MS are jointly supported by the “making connections” Weizmann-UK program. AGY further acknowledges support by a Marie Curie IRG fellowship and the Peter and Patricia Gruber Award, as well as funding by the Benozio Center for Astrophysics and the Yeda-Sela center at the Weizmann Institute. A.V.F.’s group and KAIT are supported by National Science Foundation (NSF) grant AST-0908886, the Sylvia & Jim Katzman Foundation, the Richard & Rhoda Goldman Fund, Gary and Cynthia Bengier, and the TABASGO Foundation; additional funding was provided by NASA through *Spitzer* grant 1322321, as well as *HST* grant AR-11248 from the Space Telescope Science Institute, which is operated by Associated Universities for Research in Astronomy, Inc., under NASA contract NAS 5-26555. J.S.B. and his group are partially funded by a DOE SciDAC grant. E.O.O. and D.P. are supported by the Einstein fellowship. L.B. is supported by the National Science Foundation under grants PHY 05-51164 and AST 07-07633.

We are grateful to the staff of the Gemini Observatory for their promptness and high efficiency in attending to our TOO request. Likewise, we thank the staff of the Very Large Array and the Hobby Eberly Telescope. We acknowledge the following internet repositories: SEDS (Messier Objects) and GOLDMine (Virgo Cluster). Finally, as always, we are grateful to the librarians who maintain the ADS, the NED, and SIMBAD data systems.

The Hobby-Eberly Telescope (HET) is a joint project of the University of Texas at Austin, the Pennsyl-

<sup>10</sup> Henceforth we use the term “luminous red novae” as a functional short name for such events.

vania State University, Stanford University, Ludwig-Maximilians-Universität München, and Georg-August-Universität Göttingen. The HET is named in honor of its principal benefactors, William P. Hobby and Robert E. Eberly. The Marcario Low-Resolution Spectrograph is named for Mike Marcario of High Lonesome Optics, who fabricated several optics for the instrument but died before its completion; it is a joint project of the Hobby-Eberly Telescope partnership and the Instituto de Astronomía de la Universidad Nacional Autónoma de México. *GALEX* (Galaxy Evolution Explorer) is a NASA Small Explorer, launched in 2003 April. We gratefully acknowledge NASA's support for construction, operation, and science analysis for the *GALEX* mis-

sion, developed in cooperation with the Centre National d'Etudes Spatiales of France and the Korean Ministry of Science and Technology. PAIRITEL is operated by the Smithsonian Astrophysical Observatory (SAO) and was made possible by a grant from the Harvard University Milton Fund, the camera loan from the University of Virginia, and the continued support of the SAO and UC Berkeley. The Expanded Very Large Array is operated by the National Radio Astronomy Observatory, a facility of the NSF operated under cooperative agreement by Associated Universities, Inc.

## REFERENCES

- Abazajian, K. N., et al. 2009, *ApJS*, 182, 543  
 Afşar, M., & Bond, H. E. 2007, *AJ*, 133, 387  
 Barbon, R., Ciatti, F., & Rosino, L. 1973, *A&A*, 29, 57  
 Berger, E., Kulkarni, S. R., & Chevalier, R. A. 2002, *ApJ*, 577, L5  
 Berger, E., et al. 2009, *ApJ*, 699, 1850  
 Beswick, R. J., Muxlow, T. W. B., Argo, M. K., Pedlar, A., Marcaide, J. M., & Wills, K. A. 2005, *ApJ*, 623, L21  
 Bildsten, L., Shen, K. J., Weinberg, N. N., & Nelemans, G. 2007, *ApJ*, 662, L95  
 Bloom, J. S., Starr, D. L., Blake, C. H., Skrutskie, M. F., & Falco, E. E. 2006, in *Astronomical Society of the Pacific Conference Series*, Vol. 351, *Astronomical Data Analysis Software and Systems XV*, ed. C. Gabriel, C. Arviset, D. Ponz, & S. Enrique, 751  
 Bond, H. E., Bedin, L. R., Bonanos, A. Z., Humphreys, R. M., Monard, L. A. G. B., Prieto, J. L., & Walter, F. M. 2009, *ApJ*, 695, L154  
 Bond, H. E., & Siegel, M. H. 2006, *AJ*, 131, 984  
 Boschi, F., & Munari, U. 2004, *A&A*, 418, 869  
 Botticella, M. T., et al. 2009, *MNRAS*, 398, 1041  
 Cenko, S. B., et al. 2006, *PASP*, 118, 1396  
 Chevalier, R. A., Fransson, C., & Nymark, T. K. 2006, *ApJ*, 641, 1029  
 Cohen, M., Wheaton, W. A., & Megeath, S. T. 2003, *AJ*, 126, 1090  
 Dale, D. A., et al. 2009, *ApJ*, 703, 517  
 Drake, S. A., & Ulrich, R. K. 1980, *ApJS*, 42, 351  
 Fairall, A. P. 1972, *Monthly Notes of the Astronomical Society of South Africa*, 31, 23  
 Filippenko, A. V., Li, W. D., Treffers, R. R., & Modjaz, M. 2001, in *Astronomical Society of the Pacific Conference Series*, Vol. 246, *IAU Colloq. 183: Small Telescope Astronomy on Global Scales*, ed. B. Paczynski, W.-P. Chen, & C. Lemme, 121  
 Gal-Yam, A., et al. 2004, *ApJ*, 609, L59  
 Hill, G. J., Nicklas, H. E., MacQueen, P. J., Mitsch, W., Wellem, W., Altmann, W., Wesley, G. L., & Ray, F. B. 1998, in *Society of Photo-Optical Instrumentation Engineers (SPIE) Conference Series*, Vol. 3355, *Society of Photo-Optical Instrumentation Engineers (SPIE) Conference Series*, ed. S. D'Odorico, 433  
 Holtzman, J. A., Burrows, C. J., Casertano, S., Hester, J. J., Trauger, J. T., Watson, A. M., & Worthey, G. 1995, *PASP*, 107, 1065  
 Hook, I. M., Jørgensen, I., Allington-Smith, J. R., & Davies, R. L., Metcalfe, N., Murowinski, R. G., & Crampton, D. 2004, *PASP*, 116, 425  
 Jeffery, D. J., & Branch, D. 1990, in *Supernovae, Jerusalem Winter School for Theoretical Physics*, ed. J. C. Wheeler, T. Piran, & S. Weinberg, 149  
 Kasliwal, M. M., & Kulkarni, S. R. 2010, *The Astronomer's Telegram*, 2590, 1  
 Kennicutt, Jr., R. C., et al. 2003, *PASP*, 115, 928  
 Khan, R., Stanek, K. Z., Prieto, J. L., Kochanek, C. S., Thompson, T. A., & Beacom, J. F. 2010, *ArXiv e-prints*  
 Kulkarni, S. R., & Kasliwal, M. M. 2009, in *Astronomy, Vol. 2010, astro2010: The Astronomy and Astrophysics Decadal Survey*, 165+  
 Kulkarni, S. R., et al. 2007, 447, 458  
 Law, N. M., et al. 2009, *PASP*, 121, 1395  
 Lejeune, T., & Schaerer, D. 2001, *A&A*, 366, 538  
 Li, W. D., et al. 2000, in *American Institute of Physics Conference Series*, Vol. 522, *American Institute of Physics Conference Series*, ed. S. S. Holt & W. W. Zhang, 103  
 Martin, D. C., et al. 2005, *ApJ*, 619, L1  
 Martini, P., Wagner, R. M., Tomaney, A., Rich, R. M., della Valle, M., & Hauschildt, P. H. 1999, *AJ*, 118, 1034  
 Metzger, B. D., Piro, A. L., Quataert, E., & Thompson, T. A. 2009, *ArXiv e-prints*  
 Metzger, B. D., et al. 2010, *MNRAS*, 406, 2650  
 Moriya, T., Tominaga, N., Tanaka, M., Nomoto, K., Sauer, D. N., Mazzali, P. A., Maeda, K., & Suzuki, T. 2010, *ApJ*, 719, 1445  
 Morrissey, P., et al. 2007, *ApJS*, 173, 682  
 Nugent, P. E. 2009, in *Bulletin of the American Astronomical Society*, Vol. 41, *Bulletin of the American Astronomical Society*, 419  
 Ofek, E. O., et al. 2008, *ApJ*, 674, 447  
 Oke, J. B., et al. 1995, *PASP*, 107, 375  
 Pennypacker, C. R., et al. 1989, *AJ*, 97, 186  
 Prieto, J. L., et al. 2008, *ApJ*, 681, L9  
 Rahmer, G., Smith, R., Velur, V., Hale, D., Law, N., Bui, K., Petrie, H., & Dekany, R. 2008, in *Presented at the Society of Photo-Optical Instrumentation Engineers (SPIE) Conference*, Vol. 7014, *Society of Photo-Optical Instrumentation Engineers (SPIE) Conference Series*  
 Rau, A., et al. 2009, *PASP*, 121, 1334  
 Russell, D. G. 2002, *ApJ*, 565, 681  
 Schlegel, D. J., Finkbeiner, D. P., & Davis, M. 1998, *ApJ*, 500, 525  
 Shen, K. J., Kasen, D., Weinberg, N. N., Bildsten, L., & Scannapieco, E. 2010, *ApJ*, 715, 767  
 Sheth, K., et al. 2010, *ArXiv e-prints*  
 Smith, N., et al. 2009, *ApJ*, 697, L49  
 Thompson, T. A., Prieto, J. L., Stanek, K. Z., Kistler, M. D., Beacom, J. F., & Kochanek, C. S. 2009, *ApJ*, 705, 1364  
 van Dokkum, P. G. 2001, *PASP*, 113, 1420  
 Wright, E. L., et al. 2010, *AJ*, 140, 1868